

# IMPLEMENTATION OF FAST FOCUSING ALGORITHM FOR UWB STEPPED-FREQUENCY GPR SAR IMAGING

B. Sai, J.J.M. de Wit, L.P. Ligthart

*International Research Centre for Telecommunications-transmission and Radar (IRCTR)  
Department of Electrical Engineering, Faculty of Information Technology and Systems  
Delft University of Technology, Mekelweg 4, 2628 CD Delft, The Netherlands  
E-mail: [b.sai@irctr.tudelft.nl](mailto:b.sai@irctr.tudelft.nl), [j.wit@irctr.tudelft.nl](mailto:j.wit@irctr.tudelft.nl)*

## ABSTRACT

This paper discusses a fast and efficient focusing algorithm for ultra wideband (UWB) stepped-frequency continuous-wave (SFCW) side-looking SAR image formation. Conventional SFCW SAR focusing algorithms are mostly based on the matched filter concept. Their frequency-domain implementation is burdensome. In this paper we present a more rapid and efficient algorithm for real-time and automatic UWB SFCW SAR imaging, especially for UWB ground-penetrating radar applications. The algorithm contains three key elements: two transforms and one automatic mapping of the coordinates. The processing and imaging are carried out automatically once the geometry and system parameters are given. The increased performance and efficiency of the algorithm is demonstrated using simulated UWB SFCW data acquired from a 2D target area over a 3D measurement geometry. For the raw data matrix with the size of 940 times 880 complex data points, the processing and imaging time (including upsampling procedure for data array in both range and azimuthal directions) takes 58 seconds in a Pentium III 900 MHz PC.

## INTRODUCTION

Ultra wideband (UWB) SAR at low frequency bands is getting more and more attention, since it can provide high down-range and cross-range resolutions for many applications such as geological survey, non-destructive testing and remote sensing. Conventional pulse radars however have to confront with a trade-off between large instantaneous bandwidth and high dynamic range. The stepped-frequency continuous wave (SFCW) radars can easily overcome this compromise. Furthermore, the state-of-the-art SFCW technology allows for rapid sweeping while maintaining the phase coherence. The SFCW radars are a cost-effective coherent UWB system, since they can use considerably low speed A/D conversion to fulfill UWB data acquisition. Their radiation spectrum can easily skip some interference frequencies or regulatory frequency allocation [1]. Although the SFCW systems have these advantages over pulse radars, it is a time-consuming process to obtain their high down- and cross-range resolutions by signal processing. For recently published so-called time-space algorithms derived from the  $\mathbf{w} - \mathbf{k}$  domain SAR algorithms, it is indicated that they are computationally inefficient due to the time-space domain processing [2]. In this paper we propose a more rapid and more efficient algorithm for real-time and automatic UWB SFCW SAR imaging, especially for ground-penetrating radar (GPR) applications. The frequency-domain implementation of the algorithm contains two key transforms: One is the inverse discrete Fourier transform of the complex reflectivity data to synthesize the complex range image with Hanning-window weighting. The other is the coherent integration, by means of the discrete Fourier transform, of range-resolved responses along azimuthal direction for each range cell to form the cross range image with Kaiser-Bessel windowing. The second transform leads to the demand of automatic mapping of the coordinates from the "spatial-frequency" domain to the cross-range domain. The algorithm was programmed in MATLAB<sup>®</sup>, and the processing and imaging are carried out automatically once the geometry and system parameters are given. The increased performance and efficiency of the algorithm compared to previous (ultra wideband) stepped-frequency SAR algorithms is demonstrated using simulated UWB SFCW data. The resultant SAR image formation shows all targets resolved perfectly within the ultimate resolution limits.

## SFCW WAVEFORM

UWB SFCW SAR imagery results from the data collected in the frequency domain. The transmitted frequency-stepped pulse train  $x(t)$  can be expressed as

$$x(t) = \sum_{i=0}^{N-1} A_i \cos[2\mathbf{p}(f_L + i\Delta f)t + \mathbf{q}_i] \text{rect}\left[\frac{t - iT - T/2}{T}\right], \quad (1)$$

where  $N$  is the number of frequency steps.  $\Delta f$  is the frequency step size.  $\text{rect}[\cdot]$  denotes the rectangular pulse with width  $T$ .  $\mathbf{q}_i$  is the relative phase.  $A_i$  is the amplitude of the  $i$ th pulse at frequency  $f_L + i\Delta f$ . To determine the frequency step size for unambiguously sampling a complex signal, one has to use the Nyquist's sampling criterion, which can be written as [3]:

$$\Delta f \leq \frac{v_p}{2l}, \quad (2)$$

where  $l$  is the target range extent.  $v_p$  is the propagation velocity. The spectrum of a simulated SFCW signal with 16 frequencies is shown in Fig. 1. By its nature the SFCW waveform produces a high range-sidelobe level on the synthesized range profile. Therefore, one has to use some kind of weighting functions to reduce the sidelobe level, however at the expense of degradation of range resolution [4]. We assume that  $\Gamma_1(f_k) \exp[j\mathbf{f}_1(f_k)]$  is the complex reflectivity of a point target at frequency  $f_k$  and  $\mathbf{r}_1$  is the propagation loss from the source to the point target at a distance  $r_1$ . After the reflected signal from the target is received, downconverted at the quadrature mixer with the reference signal and sampled in high instantaneous dynamic range, the complex data array at the frequency  $f_k$  can be expressed as:

$$C(f_k) = A_k \Gamma_1 \mathbf{r}_1 \exp\left[-j2\mathbf{p}f_k \frac{2r_1}{v_p} + \mathbf{f}_1\right] \quad (3)$$

## FAST UWB SAR ALGORITHM

In side-looking SAR the integration length varies with the coordinates of individual targets. We therefore use coherent integration angles rather than the integration length to avoid the cumbersome implementation. All the targets illuminated by the radar beam are observable to the radar for their aspect angles  $\in \left[-\frac{\mathbf{q}_H}{2}, \frac{\mathbf{q}_H}{2}\right]$ , where  $\mathbf{q}_H$  is the horizontal beamwidth of the radar receiving antenna. As the radar footprint passes over a target, the phase change over the two-way path from radar to the target is a function of cross range position with respect to the closest approach point. If this phase change is compensated so that the returns from a target can be constructed coherently, the energy of processed returns for the target will get focused at the closest approach point.

Range walk occurs when the range curvature exceeds one range cell due to the large bandwidth and wide beamwidth [5], which is especially true in most GPR measurements. Range walk can be examined according to

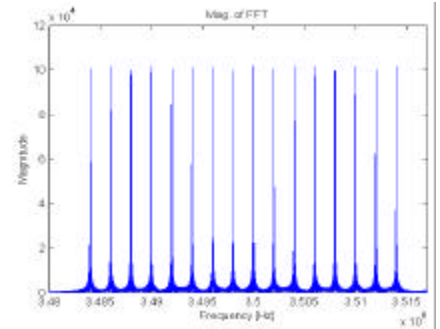


Fig. 1 Spectrum of transmitted SFCW signal at 16 frequencies

$$\mathbf{dR} = R \left\{ \left[ 1 + \left( \frac{\tan \frac{\mathbf{q}_H}{2}}{2} \right)^2 \right]^{\frac{1}{2}} - 1 \right\} \quad (4)$$

If  $dR$  is less than the slant range resolution cell size, then there is no need for range walk correction at range  $R$ . Otherwise, the range walk should be corrected by assigning the complex range-resolved responses at the respective azimuthal positions into the correct slant range cells. The slant range matrix can be expressed as:

$$\mathbf{R}_{P \times M} = \left\{ \left[ \begin{pmatrix} Laz_1 & \mathbf{K} & Laz_M \\ \mathbf{M} & \mathbf{0} & \mathbf{M} \\ Laz_1 & \mathbf{L} & Laz_M \end{pmatrix}_{P \times M} - \begin{pmatrix} y_1 & \mathbf{K} & y_1 \\ \mathbf{M} & \mathbf{0} & \mathbf{M} \\ y_P & \mathbf{L} & y_P \end{pmatrix}_{P \times M} \right]^2 + \begin{pmatrix} x_1^2 & \mathbf{K} & x_1^2 \\ \mathbf{M} & \mathbf{0} & \mathbf{M} \\ x_P^2 & \mathbf{L} & x_P^2 \end{pmatrix}_{P \times M} + H^2 \begin{pmatrix} 1 & \mathbf{K} & 1 \\ \mathbf{M} & \mathbf{0} & \mathbf{M} \\ 1 & \mathbf{L} & 1 \end{pmatrix}_{P \times M} \right\}^{\frac{1}{2}}, \quad (5)$$

where  $(x_n, y_n)$  ( $n = 1, 2, \dots, P$ ) denotes the  $n$ th grid coordinate of the target area.  $Laz_m$  ( $m = 1, 2, \dots, M$ ) are the spatial sampling positions.  $H$  is the antenna altitude. At each spatial sampling position the target area is illuminated at the  $N$  stepped frequencies,  $\mathbf{F}^T = [f_0 \ f_1 \ \mathbf{L} \ f_{N-1}]$ . The complex target range matrix can be obtained by the inverse discrete Fourier transform (IDFT) of the complex target responses, which is written as:

$$\mathbf{CF}_{N \times M} = \text{IDFT}_{\text{vs. freq.}} \left( \sum_{n=1}^P \left[ \exp \left[ -j \frac{4P}{C} [\mathbf{F}_{N \times 1}]_{I \times M \times P} \cdot [\mathbf{R}_{P \times M}^T]_{N \times I \times 1} \right] \cdot \mathbf{G}_{N \times M \times P} \right] \right), \quad (6)$$

where  $[\mathbf{R}_{P \times M}^T]_{N \times I \times 1}$  denotes a 3D slant-range matrix,  $[\mathbf{F}_{N \times 1}]_{I \times M \times P}$  is a 3D frequency matrix replicated from the frequency array,  $\mathbf{F}^T$ .  $\mathbf{G}_{N \times M \times P}$  is a 3D matrix of the measured SFCW responses from the designated target area.  $[\mathbf{A}] \cdot [\mathbf{B}]$  denotes the inner product of arbitrary  $[\mathbf{A}]$  and  $[\mathbf{B}]$ . The coherent integration of range-resolved responses along spatial sampling positions was performed by using the discrete Fourier transform (DFT) for each range cell. It is expressed as

$$\mathbf{ACF}_{N \times M} = \text{DFT}_{\text{vs. sampling positions}} \{ \mathbf{PCM}_{N \times M} \cdot \mathbf{CF}_{N \times M} \}, \quad (7)$$

where  $\mathbf{PCM}_{N \times M}$  denotes the phase correction matrix due to the range curvature and range walk. Eq. (7) leads to the need for mapping of the coordinates from the ‘‘spatial-frequency’’ domain to the cross-range domain. The automatic mapping is conducted according to

$$y = y_n + \frac{k_y x_n}{\sqrt{\left( \frac{4P}{I_c} \right)^2 - k_y^2}}, \quad (8)$$

where  $k_y$  denotes the spatial-frequency along the sampling positions. As shown in the flowchart (Fig. 2), this processing scheme allows for ultra wideband synthetic aperture processing [6].

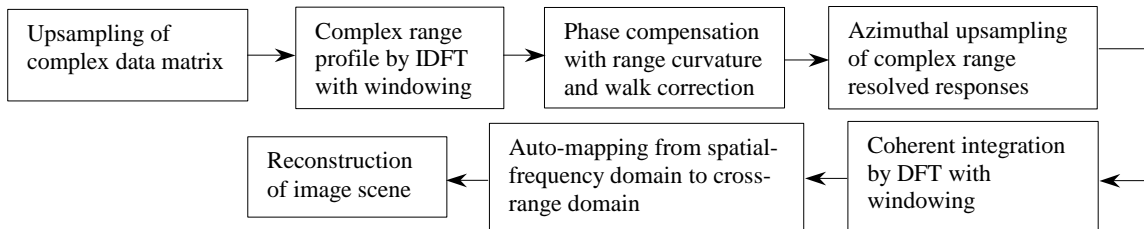


Fig. 2 Flowchart of automatic ultra wideband SAR processing

## RESULTS

The algorithm was implemented in MATLAB®. It was tested by using simulated UWB monostatic SFCW data acquired from a 2D target area over a 3D measurement geometry [Fig. 3]. The target area was formed by 9 isotropic point targets located on the  $X$ - $Y$  plane [left graph of Fig. 4]. The radar system was moved along a line at an altitude of 400 m with an antenna look angle of 14 degrees. The data was acquired in the “stop-and-go” manner. The frequency range is 256.2 MHz to 443.8 MHz. The frequency step size is 0.2 MHz. The horizontal and vertical beam-widths of the antenna are 9.9 and 45.7 deg at 350 MHz respectively. The spatial sampling interval is 0.17 m along the moving track of 150 m. The Hanning and Kaiser-Bessel windows were used to reduce the sidelobe levels in both range and azimuthal directions respectively. The right graph of Fig. 4 shows that all the targets are resolved correctly. The processing and imaging time (including upsampling procedures for the data array in both range and azimuthal directions) takes 58 seconds in a Pentium III 900 MHz PC.

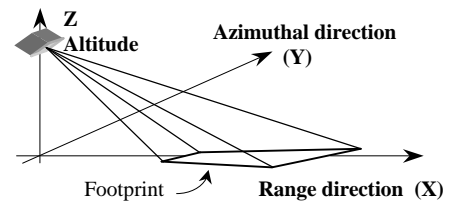


Fig. 3 Simplified geometry of Side-Looking radar

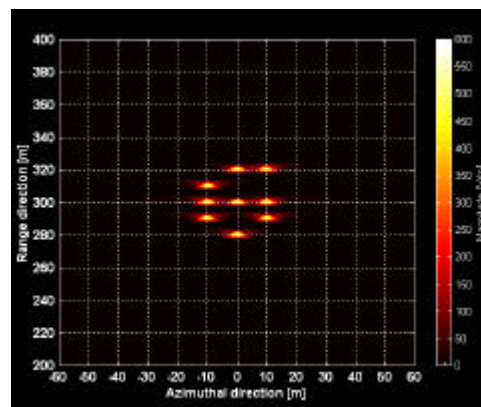
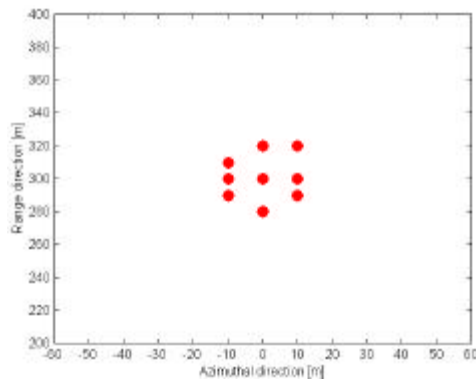


Fig. 4 Plan view of target area with 9 targets (left); Reconstruction of target scene from 3D measurement geometry (right)

## CONCLUSIONS

The algorithm is suitable for dealing with ultra wideband stepped-frequency SAR data, and works very efficiently. It can be easily adapted to the data acquired by the UWB SFCW ground-penetrating radars to make real-time/on-line imaging possible. Further tests will be performed by using real measured data on the moving platform.

## REFERENCES

- [1] US Federal Communications Commission (FCC), “NEWS Release at February 12, 2002,” Washington, D.C.,
- [2] A.U.A.W. Gunawardena, I.D. Longstaff, “Ultra-wideband widebeam SAR processing in the time-space domain,” Proc. of IEE Radar’97, pp. 229 – 232, Oct. 1997
- [3] Donald R. Wehner, “High-Resolution Radar,” Second Edition, Artech House, 1995
- [4] Fredric J. Harris, “On the use of windows for harmonic analysis with the discrete Fourier transform,” Proceeding of IEEE, vol. 66, No. 1, pp 51–83, January 1978
- [5] John C. Curlander, and Robert N. McDonough, “Synthetic aperture radar, systems and signal processing,” John Wiley & Sons, Inc., 1991
- [6] John W. McCorkle, “Focusing of synthetic aperture ultra wideband data,” Proc. of IEEE International Conference on System Engineering, Dayton, OH, USA, pp. 1-5, August 1991